The current issue and full text archive of this journal is available at
www.emeraldinsight.com/0961-5539.htm



# Evaluation of confined natural and forced convection predictions by different turbulence models

Mohamed Omri and Nicolas Galanis
*Laboratoire Thermaus, Génie Mécanique, Université de Sherbrooke, Sherbrooke, Canada*

Received 26 April 2006
Revised 18 July 2007
Accepted 12 October 2007

## Abstract

**Purpose** – The purpose of this paper is to evaluate the capacity of two equation turbulence models to reproduce mean and fluctuating quantities in the case of both natural convection and isothermal flows.

**Design/methodology/approach** – Numerical predictions of mean velocity profiles, air and wall temperatures as well as turbulent kinetic energy by three different two equation models (standard $k$-$\varepsilon$, renormalisation group $k$-$\varepsilon$ and shear-stress transport-$k$-$\omega$) are compared with corresponding experimental values.

**Findings** – The prediction of mean velocities and temperatures is in all cases satisfactory. On the other hand, the prediction of turbulent quantities is less precise.

**Originality/value** – The three models under consideration in this paper can be used for engineering applications such as HVAC calculations.

**Keywords** Turbulence, Modelling, Numerical analysis, Predictive processes, Convection, Flow

**Paper type** Research paper

## Nomenclature

$C_\mu$ = empirical constant in turbulence model
$C_p$ = specific heat
$g$ = gravitational acceleration
$H$ = height of cavity
$h$ = height of the inlet (forced convection)
$K$ = thermal conductivity
$k$ = turbulent kinetic energy
$K_{\text{eff}}$ = effective thermal conductivity
$L$ = length of cavity
$p$ = pressure
$Ra$ = Rayleigh number, $Ra = g\beta\Delta T H^3/(\alpha\nu)$
$Re_y$ = turbulent Reynolds number based on $y = yk^{\frac{1}{2}}/\nu$
$Re$ = Reynolds number
$R_t$ = turbulent Reynolds number
$S_{ij}$ = large scale strain rate
$T$ = temperature
$t$ = height of the outlet (forced convection)
$T_c$ = cold wall temperature
$T_h$ = hot wall temperature
$v$ = velocity component in $y$-direction (natural convection)
$u$ = velocity component in $x$-direction (natural convection)
$U$ = velocity component in $x$-direction (forced convection)
$U_{\text{in}}$ = velocity inlet (forced convection)
$V_0$ = buoyancy velocity, $V_0 = \sqrt{g\beta H(T_h - T_c)}$
$W$ = width of cavity
$w$ = width of the inlet (forced convection)
$x_i$ = Cartesian space coordinates ($i = 1, 2, 3$)

The authors thank the Natural Sciences and Engineering Research Council of Canada for its financial support.

International Journal of Numerical Methods for Heat & Fluid Flow
Vol. 19 No. 1, 2009
pp. 5-24

0961-5539
DOI 10.1108/09615530910922125

*Greek symbols*

$\alpha$ = thermal diffusivity
$\beta$ = thermal expansion coefficient
$\Delta T$ = temperature difference $\Delta T = (T_h - T_c)$
$\varepsilon$ = dissipation rate of $k$
$\nu$ = kinematic viscosity
$\nu_t$ = turbulent viscosity, $\nu_t = C_\mu k^2/\varepsilon$
$\rho$ = fluid density
$\tau_w$ = wall shear stress
$\omega$ = specific dissipation rate of $k$

*Subscripts*

LRN = low Reynolds number
RNG = re-normalisation group
SST = shear stress transport
enh = enhanced
wf = wall function

## 1. Introduction

Confined turbulent flows occur in many natural situations and industrial applications. Increasingly, such flow fields are analysed using CFD codes with various turbulence models of different complexity. Evidently, the usefulness of such codes is conditioned by their capacity to reproduce experimental data. Two types of confined flows have been used extensively for such comparisons: the buoyancy-driven flow in an enclosure with differentially heated vertical walls (natural convection) and the isothermal forced flow in an air filled cavity.

Natural convection in differentially heated enclosures constitutes a reference problem used extensively to test and evaluate different models and solution algorithms included in CFD codes. Thus, Peng and Davidson (2000) investigated the performance of low Reynolds number (LRN) $k$-$\omega$ models for predicting buoyancy affected flows in cavities by comparison with LRN $k$-$\varepsilon$ models and with experiments. They reported that for natural convection in a tall cavity with $Ra = 5 \times 10^{10}$ none of the analysed models were able to produce a grid-independent solution. This problem was eliminated by introducing a damping function into the buoyant source term in the $k$-equation. Liu and Wen (1999) developed a buoyancy-modified turbulence model based on the four-equation model ($(k - \varepsilon - \overline{\theta^2} - \varepsilon_\theta)$) and tested it in buoyancy-driven cavity flows by comparison with experimented data and the predictions from three other turbulence models. They reported that this model demonstrated significant improvements in capturing the anisotropy of Reynolds stresses and turbulent heat flux in vertical boundary layers. Peng and Davidson (2001) investigated the buoyant flow in a cavity for a relatively low-turbulence level ($Ra = 1.58 \times 10^9$) by means of large eddy simulation. The numerical predictions for the mean flow quantities are in good agreement with experimental values but less accurate for turbulence statistics, particularly in the outer region of the near-wall flow where the boundary layer interacts with the recirculating core region. Dol and Hanjalic (2001) studied turbulent natural convection in a near-cubic enclosure at high-Rayleigh number ($Ra = 4.9 \times 10^{10}$). The turbulence models used to close the RANS equations were a LRN $k$-$\varepsilon$ model and a second-moment closure (SMC). Their results showed that the SMC was better in capturing thermal three-dimensionality effects and strong streamline curvature in the corners. The LRN $k$-$\varepsilon$ model provided reasonable predictions of the first moments away from the corners. Recently, Joubert *et al.* (2005) compared the prediction of seven different modelling approaches for turbulent natural convection and pollutant diffusion in a 2D partially partitioned cavity. They reported significant differences between the predictions for mean temperature, velocity and kinetic energy profiles. The corresponding computed Nusselt numbers at the walls lie within a $\pm 25$ per cent range.

Similarly, isothermal forced flow in an air filled cavity has also been studied extensively with CFD codes. Chen and Xu (1998) applied a zero equation model in order to simulate indoor airflow. They indicated that the zero equation model requires less computing time than the $k$-$\varepsilon$ models but its predictions are far from the experimental data of Nielsen *et al.* (1978) when the inlet width is comparable to that of the cavity. Chen (1995) applied five different low-Reynolds number two equation models in order to predict forced convection in a room; the Reynolds number at the inlet is 5,000. Their predictions for the mean velocity agree broadly with the experimental data except for those obtained by the two scale model. However, Chen considered that the flow is 2D whereas the large eddy simulation of Davidson and Nielsen (1996) for the same room indicated that it is 3D. Later, Chen (1996) applied three second order turbulent models (Reynolds stress models) to predict air motion in the same room. His comparisons of the predicted mean velocity with experimental data indicated that even the second order models do not reproduce quantitatively the measured velocity profiles. Davidson and Nielsen (1996) used large eddy simulation with two different subgrid models in the 3D ventilated cavity tested by Nielsen *et al.* (1978). They stated that the simple Smagorinsky model was inadequate because of its dependence on the Smagorinsky constant. On the other hand, the dynamic model predictions were in good agreement with experimental data. It should be noted that none of these studies, which practically considered all the levels of turbulence modelling, succeeded to reproduce quantitatively the totality of the available experimental data. From an engineering point of view, however, these predictions provide a good description of the simulated airflow.

This methodology, i.e. the comparison of CFD predictions with experimental results for either natural convection or isothermal forced flows, can lead to the selection of different "best" models for each type of flow. However, in the case of HVAC applications in buildings, the situation is more complex because of the variable operation and dispersed character of heat sources and ventilation inlets. Thus, at any given moment, the flow field can be dominated by forced convection in one part of the building and by natural convection in another. Furthermore, in the same part of the building forced convection dominates when the ventilation is on but natural convection becomes predominant when it is turned off. It is therefore clear that, in order to simulate such complex conditions, the flow model must be very robust and capable of simulating equally well both natural convection and isothermal forced flows.

In view of this situation, the present study has been undertaken to evaluate the capacity of two equation turbulence models to reproduce mean and fluctuating quantities in the case of both natural convection and isothermal flow with the smallest possible discretization grid. Specifically, three models are considered: the well known $k$-$\varepsilon$ by Launder and Spalding, the re-normalization group (RNG) $k$-$\varepsilon$ formulation which is widely used for engineering studies and the shear-stress transport (SST) $k$-$\omega$ model. In order to determine the accuracy of the wall shear stress predictions two different near wall formulations are associated with each of the two $k$-$\varepsilon$ models. The first one is the standard wall function (near wall modelling) which introduces the effect of turbulent viscosity starting from the first node of calculation. The second near wall formulation combines the one equation model of Wolfstein (1969) near the wall to each $k$-$\varepsilon$ model. The evaluation is carried out by comparing numerical predictions of mean velocity and temperature profiles, as well as turbulent quantities, with published

experimental results for a differentially-heated cavity by Ampofo and Karayiannis (2003) and for a ventilated isothermal cavity by Nielsen *et al.* (1978). The results presented here are different and more detailed than our conference presentations (Omri and Galanis, 2006a, b).

## 2. Description and modelling of the problem

The natural convection field used for validation was measured by Ampofo and Karayiannis (2003) in an air-filled cavity with identical width and height ($W = H = 0.75$ m) and a depth of 1.5 m. The isothermal vertical walls at $x = 0$ and $x = 0.75$ m were maintained at $T_h = 50 \pm 0.15$°C and $T_c = 10 \pm 0.15$°C, respectively. The corresponding Rayleigh number is $1.58 \times 10^9$. The top and bottom walls at $y = 0$ and 0.75 m were made from 1.5 mm mild steel plates, insulated on the outside with polystyrene and wood. The temperature of the surrounding air was controlled at $30 \pm 0.2$°C which is equal to the average of the hot and cold walls temperatures. Through a well-controlled experimental setup, it was claimed that the flow field is 2D in the middle of the spanwise direction where the measurements were made. It should be noted that the dimensions of this cavity and the experimental conditions are identical to those used by Peng and Davidson (2001) to validate their LES calculations. Therefore, it is also possible to compare their numerical predictions with the present ones.

The forced convection field used for validation was measured by Nielsen *et al.* (1978) in an air-filled parallelepipedic cavity with identical width and height ($W = H = 89.3$ mm) and a length $L = 3H = 258.9$ mm. The air inlet was centred near the top of one of the shorter walls at $x = 0$. Its width and height were $w = 0.5\,W$ and $h = 0.056\,H$, respectively. The air outlet was near the bottom of the opposite short wall at $x = L$. Its width was equal to $W$ and its height $t = 0.16\,H$. The Reynolds number based on the inlet velocity and inlet height is 5,000.

For both geometries the $xOz$ plane coincides with the horizontal floor of the cavity and gravity acts in the negative $y$-direction.

The flow field in these cavities is modelled with the Reynolds averaged Navier-Stokes equations. The molecular transport properties of the air are assumed to be constant. Thus, the RANS equations for mass momentum and energy are:

$$\frac{\partial}{\partial x_i}(u_i) = 0 \tag{1}$$

$$\frac{\partial}{\partial x_j}(u_j u_i) = -\frac{1}{\rho}\frac{\partial p}{\partial x_i} + \frac{\partial}{\partial x_j}\left((\nu + \nu_t)\frac{\partial u_j}{\partial x_j}\right) + \beta(T - T_0)g_i \tag{2}$$

$$\mathrm{u_j}\frac{\partial}{\partial x_\mathrm{j}}(\rho C_p T) = \frac{\partial}{\partial x_\mathrm{i}}\left(K_{\mathrm{eff}}\frac{\partial T}{\partial x_i}\right) \tag{3}$$

In the case of the natural convection field the conduction equation is also solved in the top and bottom three-layer walls with a uniform convection coefficient applied between their outer surface and the surrounding air at 30°C. On their inside surface, the air and steel temperatures as well as the corresponding heat fluxes are equal. The thermal conditions at $x = 0$ and0.75 m are $T_h = 50$°C and $T_c = 10$°C, respectively.

In the case of the isothermal forced flow only the continuity and momentum equations are necessary since $T = T_0$ and the last term in equation 2 is zero.

The turbulence models used to close the RANS equations are the standard $k$-$\varepsilon$ (Launder and Spalding, 1974), RNG $k$-$\varepsilon$ (Yakhot and Orszag, 1986) and SST-$k$-$\omega$ (Menter, 1993, Menter *et al.*, 2003) models. The reasons for these choices and the principal characteristics of the models are:

- The standard $k$-$\varepsilon$ model (Launder and Spalding, 1974) is well documented in the literature. It is simple to implement and very robust. Among the many numerical studies using this model, it is worth mentioning a recent analysis of turbulent flow with heat and mass transfer in ice rinks (Bellache *et al.*, 2005).
- The RNG $k$-$\varepsilon$ model has been used extensively in HVAC studies (Chen, 1995; Posner *et al.*, 2003; Dechang *et al.*, 2005). It is similar to the standard $k$-$\varepsilon$ model with an additional term in the dissipation rate equation. The constants of the model were determined using the renormalisation group theory (Yakhot *et al.*, 1992). It includes the effect of swirl on turbulence, thus enhancing its accuracy for such flows.
- The SST-$k$-$\omega$ model is an amelioration of the Wilcox $k$-$\omega$ model (Wilcox and Traci, 1976). The latter is accurate for boundary layer flows (Shpak, 1994) with moderate adverse pressure gradients but fails for flows with pressure induced separation (Menter, 1993). On the other hand, the SST-$k$-$\omega$ model has been used successfully to predict flows with strong adverse pressure gradients and separation (Menter *et al.*, 2003). It is therefore expected to be particularly suited for the isothermal flow with extensive reverse flow described by Nielsen *et al.* (1978). Moreover, this model is a weakly non-linear model since the value of $C_\mu$ in the turbulent viscosity depends on the turbulence field (Quéré *et al.*, 2003).

The SST-$k$-$\omega$ model takes into account the effects of wall proximity. On the other hand, the $k$-$\varepsilon$ models are primarily valid for turbulent core flows. For the near-wall region, they use empirical laws to express the mean velocity parallel to the wall and the turbulence quantities outside the viscous sub-layer in terms of the distance from the wall and wall conditions (such as wall shear stress and wall heat flux). Hence, the wall functions can be used to provide near-wall boundary conditions for the momentum and turbulence transport equations, rather than conditions at the wall itself, so that the viscous sub-layer does not have to be resolved and the need for a very fine mesh is circumvented. The commercial code used to solve this system of PDEs (Fluent, 2005) offers the possibility of using standard wall functions or enhanced wall treatment.

The standard wall functions are based on the proposal of Launder and Spalding (1974) and have been used widely for industrial flows. The variation of both mean velocity and temperature is linear in the viscous sub-layer and logarithmic in the region where turbulence dominates. In the commercial code used for the present study (Fluent, 2005) these functions are expressed in terms of the following variables:

$$y^* = \frac{\rho C\mu^{0.25} k_p^{0.5} y_P}{\mu} \quad U^* = \frac{u_P C_\mu^{0.25} k_p^{0.5}}{\tau_w/\rho} \tag{4}$$

where $P$ is the grid point nearest to the wall. In the viscous sublayer (i.e. for $y^* < 11.225$) the appropriate relation is:

$$U^* = y^* \tag{5a}$$

while the logarithmic law expressed as:

$$U^* = \frac{\ln(9.793y^*)}{0.4182}, \tag{5b}$$

is applied for $y^* > 11.225$. These relations show that the velocity near the wall depends on the local value of the turbulent kinetic energy. Therefore, for the $k$-$\varepsilon$ models (with the option to obtain wall boundary conditions from the $k$ equation enabled) the $k$ equation is solved in the whole domain including the wall adjacent cells. The solution of this equation requires the production and dissipation of $k$ which are, respectively, derived from the wall shear stress and from the local equilibrium hypothesis (near the wall the production of k is equal to the dissipation rate). The boundary condition imposed at the wall is *(k*/(*n* where $n$ is the distance normal to the wall.

The enhanced wall treatment is a near wall modelling that combines the enhanced wall functions proposed by Kader (1981) with a two layer model. Specifically, it uses the one equation model of Wolfstein (1969) in the near wall region and the $k$-$\varepsilon$ in the fully turbulent region. The demarcation of the two regions is determined by a wall-distance-based, turbulent Reynolds number, defined as $Re_y = yk^{1/2}/v$. The region is fully turbulent when $Re_y > 200$.

Therefore, this study uses four different combinations of turbulence models and near-wall treatments as well as the shear stress model of Menter *et al.* (2003). They are identified as $k$-eps-wf ($k$-$\varepsilon$ with standard wall functions), $k$-eps-enh ($k$-$\varepsilon$ with enhanced wall treatment), $k$-rng-wf ($k$-$\varepsilon$ RNG with standard wall functions), $k$-rng-enh ($k$-$\varepsilon$ RNG with enhanced wall treatment) and SST-$k$-$\varepsilon$ (shear stress model).

## 3. Numerical solution

The coupled elliptic PDEs describing the flow field were discretized with the finite volume method. The rectangular staggered grid is non-uniform in all directions: it is finer near the walls where gradients are more important. Second order central discretization is used, except for the convection terms where the third order Monotone Upstream-Centered Schemes for Conservation Laws (MUSCL) is applied. This third-order convection scheme (van Leer, 1979) was conceived from the original MUSCL by blending a central differencing scheme and a second order upwind scheme. Compared to the second-order upwind scheme, it can improve spatial accuracy by reducing numerical diffusion and is available for all transport equations.

Grid independence was tested for each of the five combinations of turbulence models and wall treatments by monitoring the variables and residuals during the iteration process and by refining the non-uniform grid for the two flow cases under consideration.

For the 2D natural convection case four grids have been tested. Typical results are shown in Figure 1(a) and in an earlier text (Omri and Galanis, 2006a). They indicate that the maximum difference between k values predicted by the $30 \times 30$ and $150 \times 150$ grids is an acceptable 2.5 per cent. The corresponding differences for mean velocity components and temperature are even lower as established by Peng and Davidson (2001) for low-turbulence-level flows. It must be noted that the grid independence tests shown in Figure 1 are more rigorous than corresponding tests which compare mean velocity or temperature predictions since turbulent kinetic energy is more sensitive to the number and distribution of the discretization nodes (Peng and Davidson, 1988). In view of such results further calculations for this case have been performed with the $30 \times 30$ grid.

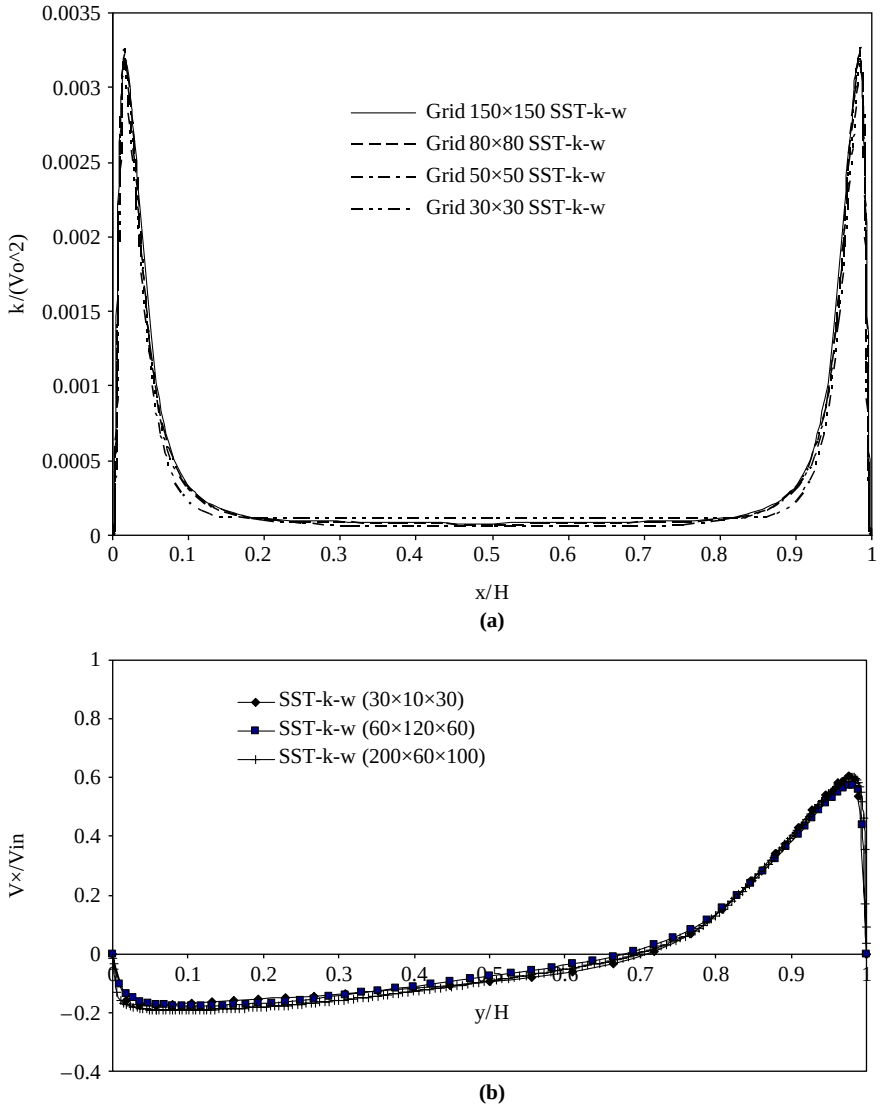


**Figure 1.**
Grid independence tests: 1a/Turbulent kinetic energy for natural convection at $y/H = 0.5$; 1b/Horizontal velocity for isothermal flow at $x/H = 2$, $z/H = 0$

For the 3D forced convection case, grid independence was tested in an earlier study (Omri and Galanis, 2006b) for each of the five combinations of turbulence models and wall treatments by comparing results calculated with four different grids (30 × 10 × 30, 60 × 10 × 30, 30 × 20 × 30 and 30 × 10 × 60 nodes in the $x$, $z$, and $y$-directions, respectively). The small number of grid points in the $z$-direction, which is used to illustrate that the flow is 3D, was based on the fact that many previous numerical studies of this flow field (Nielsen *et al.*, 1978; Chen and Xu, 1998; Mora *et al.*, 2003) have obtained satisfactory results with a 2D representation. The number of grid points in these three studies varies from a very coarse grid (6 × 6 used to compare its

predictions with those of a zonal model) to a "fine" grid (40 × 40). In particular, Nielsen *et al.* (1978) used two grids (17 × 20 and 39 × 39) and reported differences of up to 3 per cent between their predictions. They stated "that the magnitude of uncertainty is likely to remain with all practically possible numbers of grid nodes". In view of this situation the number of nodes in the four grids used earlier is reasonable. However, for the present purposes three more grids (30 × 10 × 30, 60 × 20 × 60 and 200 × 60 × 100) have been evaluated. Their predictions of average velocity profiles at the three different positions where corresponding experimental results are available were used to evaluate their effect. Particular emphasis was placed on the magnitude and position of the maximum jet velocity as well as on the extent and intensity of the experimentally determined reverse flow. Some results of these comparisons are shown in Figure 1(b) which clearly shows that the numerical predictions with these three grids are essentially the same. Based on these comparisons all the results for this case presented here have been calculated with 30 × 30 × 10 nodes. The distribution of these nodes is such that the calculation domain contains 6 × 6 nodes *vis-à-vis* the inlet ($|z| < w/2$ and $H - h < y < H$). However, at the inlet itself ($x = 0$) the resolution was increased by adding six additional nodes in both the $y$ and $z$-directions.

As shown in the next sections, these grids provide numerical predictions comparable to those reported in other numerical studies and in good agreement with measured values. Therefore, the chosen discretization is perfectly adequate for engineering calculations such as those related to HVAC applications.

## 4. Results and discussion

### *4.1 Natural convection*

*4.1.1 Mean velocity and mean temperature predictions*. The non-dimensional mean temperature profiles and the profiles of the non-dimensional mean vertical velocity calculated by each of the five models under consideration are qualitatively similar. They indicate that the flow field consists of a relatively narrow boundary layer along the vertical walls and a nearly stagnant core region (from $x/H \approx 0.15$ to $x/H \approx 0.85$) where the temperature decreases almost linearly as the distance from the hot wall increases. All these numerical results are in as good agreement with the corresponding measured values as those calculated with LES by Peng and Davidson (2001). However, this agreement is not uniform throughout the cavity. Thus, Figure 2 shows that all five models give essentially the same temperature profiles at mid-height ($y/H = 0.5$) but predict very different temperatures at $y/H = 0.2$ and 0.8. This observation indicates the importance of extending the comparisons to the entire cavity, in particular to see the effect of the horizontal boundary layers along the top and bottom walls. Near the bottom of the cavity and at mid-height they all under predict the temperature in the core region ($0.15 < x/H < 0.85$). Near the top, the $k$-eps-wf under predicts slightly the core temperature while the two formulations using the enhanced wall treatment over predict this temperature. In the ascending boundary layer, the agreement between calculated and measured values is fairly good at mid-height, even if $k$-$\varepsilon$-enh, $k$-$\varepsilon$-RNG-enh and SST-$k$-$\omega$ slightly under predict the dimensionless temperature near $x/H = 0.01$. Near the bottom of the cavity the calculated values in the boundary layer do not agree as well with the measurements. At this last position the $k$-eps-wf over predicts the air temperature while the two formulations using the enhanced wall treatment under predict it. Near the top of the cavity the $k$-rng-wf provides the best prediction of the increasing temperature near the hot wall.

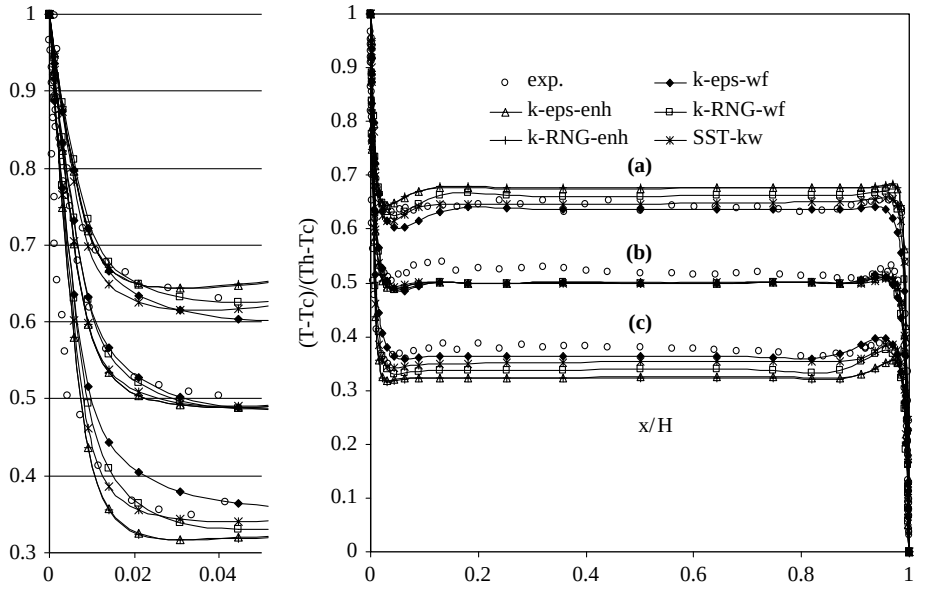


**Figure 2.**
Thermal boundary layer near the hot wall at three different heights: (a) $y/H = 0.8$; (b) $y/H = 0.5$; (c) $y/H = 0.2$ (natural convection)

Figure 3 shows that all five formulations give identical predictions for the vertical velocity in the core region and are in excellent agreement with the corresponding measured values. On the other hand, in the ascending boundary layer their predictions differ considerably. At $y/H = 0.2$ the $k$-rng-wf gives the best estimate of the increasing velocity. However, at this height all five models over predict the position of the maximum velocity. At the two other heights the position of the maximum is predicted satisfactorily by all models. At mid-height, both the $k$-$\varepsilon$ and the $k$-RNG models associated with the wall function correction overestimate the thickness of the boundary layer and the magnitude of the dimensionless velocity for $0.03 < x/H < 0.06$. On the other hand, the three other formulations ($k$-$\varepsilon$-enh, $k$-$\varepsilon$-RNG-enh and SST-$k$-$\omega$) underestimate the dimensionless velocity for $0.01 < x/H < 0.025$ but provide a good estimate of the boundary layer thickness at this height. It should be noted that the $k$-eps-wf model over predicts the increasing velocity at all heights while the two formulations using the enhanced wall treatment under predict this velocity at all three heights. As a result the former over predicts the thickness of the boundary layer while the other two underestimate it. The work of Holling and Herwig (2005), who proposed new boundary layer laws for natural convection, is particularly significant in light of these results.

It is particularly important to note that the two formulations using the enhanced wall treatment give identical results for both the temperature and velocity at all three heights. This result is due to the fact that the level of turbulence is quite low in this particular case (Peng and Davidson, 2001) so that $Re_y < 200$. Consequently, it is the one equation model which is applied throughout the domain in this particular case and the distinction between $k$-eps-enh and $k$-rng-enh is meaningless for this flow.

Figure 4 compares the calculated non-dimensional temperature of the two horizontal walls with the corresponding measurements. Overall, the $k$-$\varepsilon$-wf formulation gives the best estimates, especially near the hot side ($x/H = 0$) of the bottom wall and

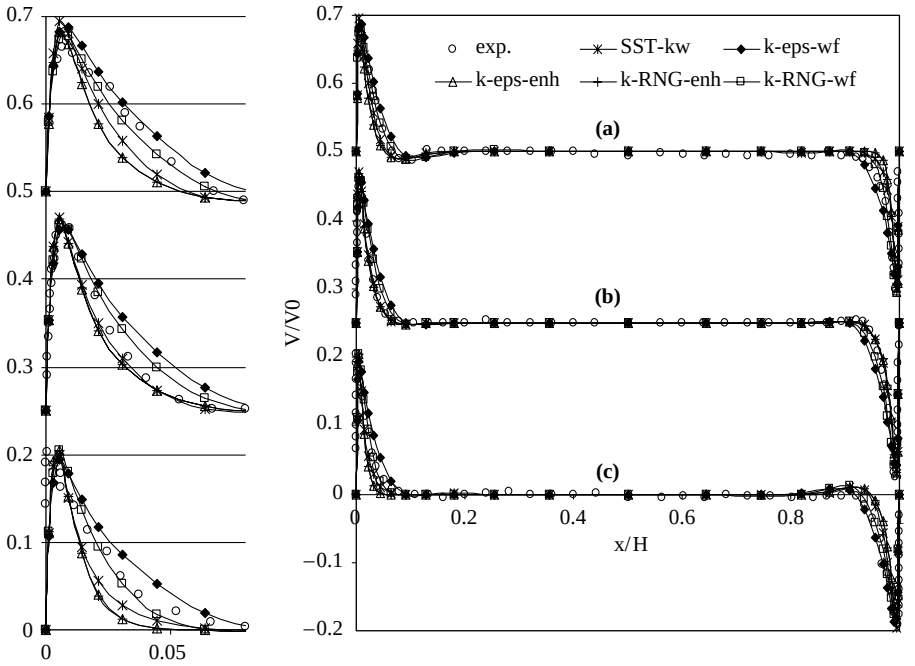


**Figure 3.**
Hydrodynamic boundary layer near the hot wall at three different heights: (a) $y/H = 0.8$; (b) $y/H = 0.5$; (c) $y/H = 0.2$ (natural convection)

near the cold side ($x/H = 1$) of the top wall where the temperature gradients are highest. It is followed by $k$-$\varepsilon$-RNG-wf, SST-$k$-$\omega$, and the two models using the enhanced wall treatment. All five formulations fail to reproduce the data for the top wall near the hot side ($x/H = 0$). In this region, the temperature is overestimated by almost 2°C by all five models while the difference between their predictions is less than 0.5°C. This observation is consistent with the remark by Peng and Davidson (2001) who indicated that, contrary to LES, two equation models do not reproduce accurately the flow details in the corners of the cavity. It should also be mentioned that radiative exchanges between the inside surfaces of the cavity (which have not been included in any of the studies mentioned in the present paper) would tend to lower the temperature of the top wall and increase that of the bottom one. Thus, the inclusion of radiation would likely reduce the differences between the measured and calculated values in Figures 2 and 4.

Finally, Figure 5 compares calculated and measured mean air temperatures at the mid-section ($x/H = 0.5$) of the cavity. It is clear that the $k$-$\varepsilon$-wf and SST-$k$-$\omega$ formulations give the best predictions. On the other hand, the two formulations using the enhanced wall treatment and the $k$-$\varepsilon$-RNG-wf model give the least satisfying predictions of this variable. With respect to this temperature profile it is important to mention that the two inflexion points near the upper and lower walls are a result of the fact that these walls are conductive. Indeed, numerical studies (Aounallah *et al.*, 2005) which consider that the inner surface of these walls are adiabatic obtain a monotonically increasing temperature distribution from $y/H = 0$ to 1.

*4.1.2 Turbulence quantities*. Figure 6 shows the experimental values of the non-dimensional turbulent kinetic energy at three heights of the cavity with

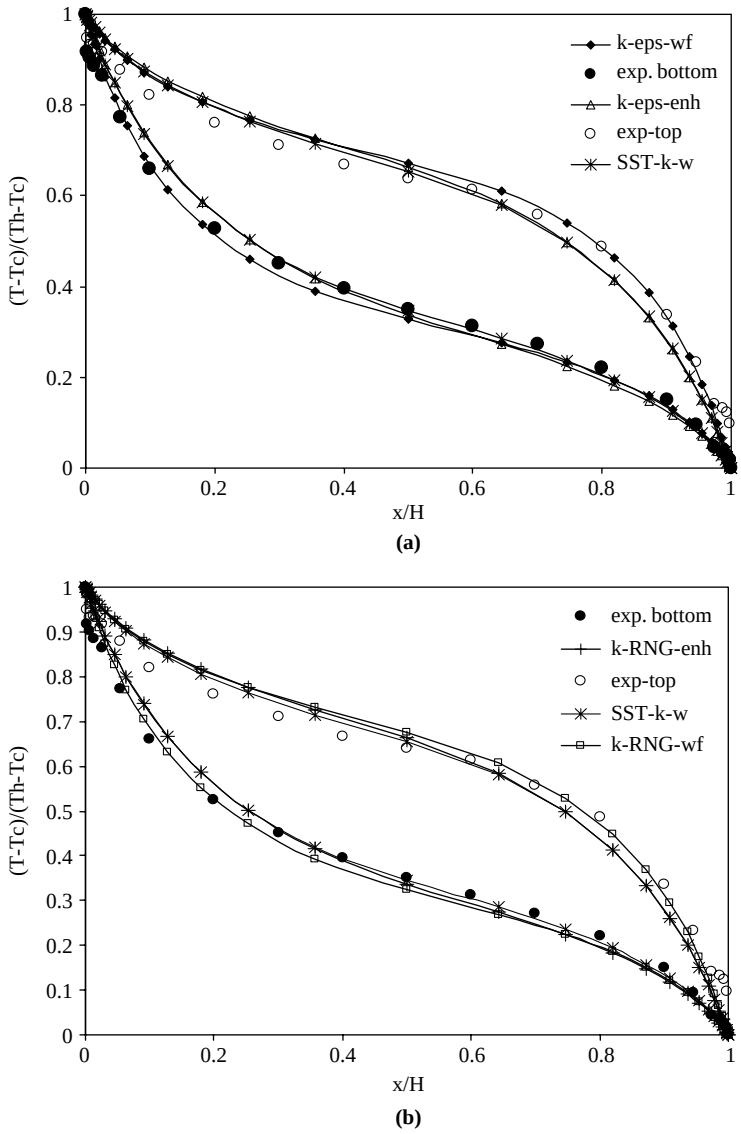


**Figure 4.**
Temperature distribution along the horizontal walls (natural convection)

corresponding numerical results. It should be noted that the two wall function formulations ($k$-$\varepsilon$-wf and $k$-$\varepsilon$-RNG-wf) do not reproduce correctly the asymptotic behaviour of $k$ near the walls since these wall functions assume a constant value of $\tau_w$ throughout the viscous sublayer. Thus, they predict that $k \neq 0$ at the walls. On the other hand, the other three formulations ($k$-$\varepsilon$-enh, $k$-$\varepsilon$-RNG-enh and SST-$k$-$\omega$) give $k = 0$ at the walls and a nearly parabolic profile ($k \sim y^2$) near the walls. This last prediction is in agreement with the corresponding result for the boundary layer of a flat plate (Speziale *et al.*, 1992).

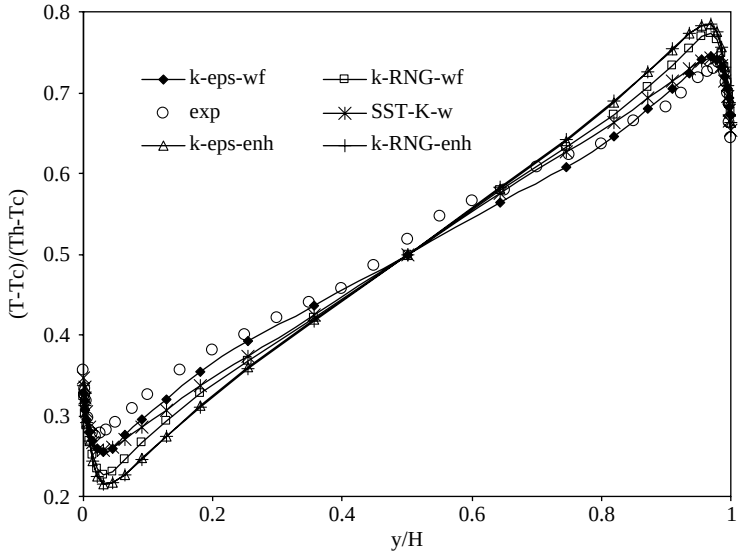


**Figure 5.**
Temperature distribution at $x/H = 0.5$ (natural convection)

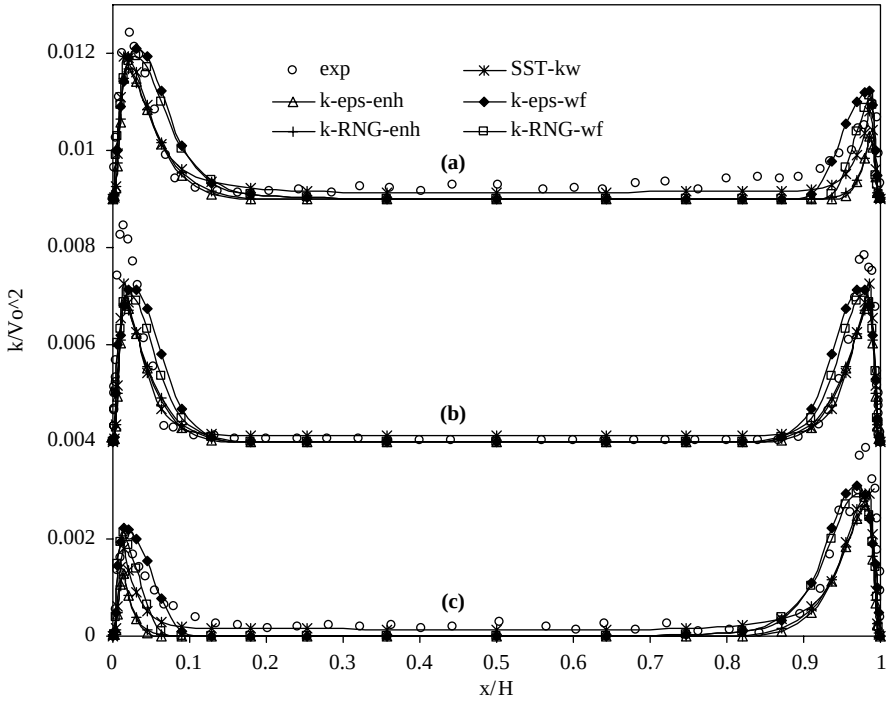


**Figure 6.**
Turbulent kinetic energy at three different heights: (a) $y/H = 0.8$; (b) $y/H = 0.5$; (c) $y/H = 0.2$ (natural convection)

Figure 6 shows that at mid-height the measured values near the hot and cold walls are not equal unlike the calculated results. It also indicates that the predicted maxima of $k/V_0^2$ are in all cases considerably lower than the corresponding experimental results and their predicted position is further away from the hot wall than the corresponding measured values. Table I shows the maximum value of $k/V_0^2$ and its position as calculated by each of the five formulations used here as well as the corresponding results of LES calculations by Peng and Davidson (2001) and experimental data. It is clear that the SST-$k$-$\omega$ gives the best estimate of the maximum value while all the other formulations, including LES, predict a value approximately 30 per cent below the experimental result. The SST-$k$-$\omega$ and the two formulations using the enhanced wall treatment give a good estimate for the position of the maximum value. On the other hand, the $k$-$\varepsilon$-wf, $k$-$\varepsilon$-RNG-wf and LES of Peng and Davidson (2001) overestimate this position by approximately 50 per cent. Based on a combination of these observations, the best performance at mid-height is obtained by the SST-$k$-$\omega$ model followed by the two formulations using the enhanced wall treatment.

At the other two heights ($y/H = 0.2$ and 0.5) the two formulations using the enhanced wall treatment give the best estimate of $k$ in the core region. On the other hand, none of the five formulations under consideration give an entirely satisfactory representation of the $k$ profile near the hot and cold walls for these two heights. Near the bottom left corner and the top right corner of the cavity the predicted increase of $k$ from its very small core value is much steeper than the corresponding measured gradient. However, at these two positions the maximum values of $k$ predicted by all five models are in fairly good agreement with the corresponding measured values. On the other hand, near the top left corner and the bottom right corner (where values of $k$ are higher than at the other two corners) the predicted gradient of $k$ is closer to the experimental result. However, at these two positions the maximum values of $k$ predicted by all five models are smaller than the corresponding measured values.

*4.2 Isothermal flow*

*4.2.1 Mean velocity predictions*. Figure 7 shows the measured and calculated horizontal component of the velocity at two different distances from the air inlet in the symmetry plane ($z = 0$) of Nielsen *et al.*'s (1978) parallelepipedic cavity.

Figure 7(a) shows the results at $x/H = 1$ calculated with the $k$-$\varepsilon$ model. They show that the two wall treatments under consideration do not have any significant influence on the calculated velocity profile, except in the lower part of the cavity where they both

| | Exp. data Ampofo and Karayiannis (2003) | LES (Peng and Davidson, 2001) | SST-$k$-$\omega$ | $k$-$\varepsilon$-enh | $k$-$\varepsilon$-RNG-enh | $k$-$\varepsilon$-wf | $k$-$\varepsilon$-RNG-wf |
|---|---|---|---|---|---|---|---|
| Max. of $k/V_0^2$ | 0.00445 | $\approx 0.0038$ * | 0.0032 | 0.0029 | 0.0029 | 0.0031 | 0.003 |
| Position of max $k/V_0^2$ | 0.0133 | $\approx 0.013$ * | 0.014 | 0.014 | 0.014 | 0.021 | 0.021 |

**Note:** *These are approximate values obtained by digitalizing graphical data in Peng and Davidson (2001)

**Table I.** Comparisons of turbulence quantities (natural convection) at mid-height

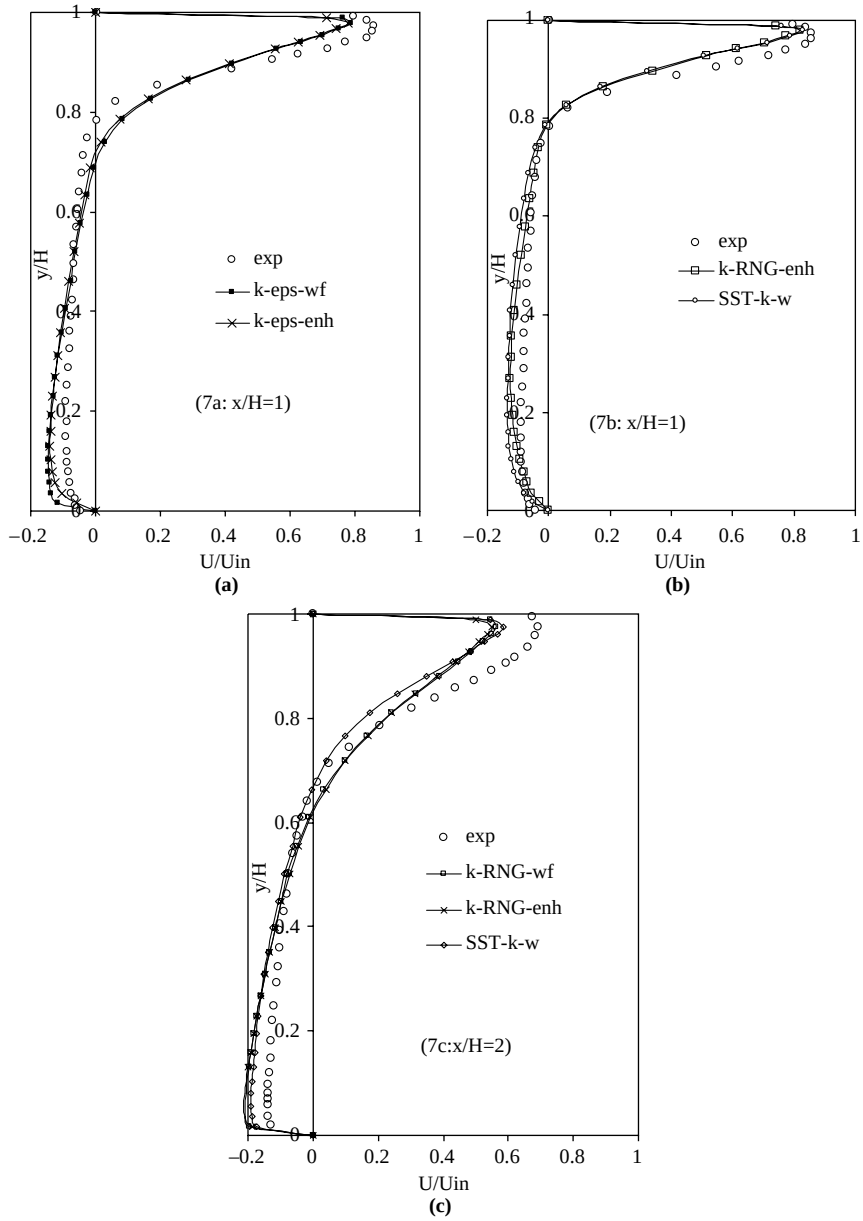


**Figure 7.**
Horizontal velocity profiles at $z/W = 0$ (isothermal flow)

overestimate the importance of the backflow. It is noted that the numerical results underestimate the peak jet velocity and overestimate its width. The corresponding results calculated with the $k$-$\varepsilon$-RNG-wf (not shown here for lack of space) and $k$-$\varepsilon$-RNG-enh (Figure 7(b)) formulations give better estimates of both the peak jet

velocity and its width. However, the $k$-$\varepsilon$-RNG-wf overestimates considerably the importance of the backflow for $y/H < 0.3$. Thus, the differences between the two wall treatments under consideration are more pronounced in the case of the $k$-$\varepsilon$-RNG model than in the case of the standard $k$-$\varepsilon$ model. Finally, the corresponding profile predicted by the SST-$k$-$\omega$ model (Figure 7(b)) is for all practical purposes identical to the one predicted by the $k$-$\varepsilon$-RNG-enh formulation. These two profiles are the closest to the measured one. The corresponding predictions of 3D LES with a $102 \times 52 \times 52$ mesh (Davidson and Nielsen, 1996) give a good estimate of the maximum jet velocity but underestimate considerably its width. They also underestimate considerably the negative velocities (reverse flow) for $y/H < 0.15$.

Figure 7(c) shows analogous results further away from the air inlet ($x/H = 2$) calculated with the $k$-$\varepsilon$-RNG-wf, $k$-$\varepsilon$-RNG-enh and SST-$k$-$\omega$ formulations. It is again noted that all three formulations underestimate the peak jet velocity. However, the SST-$k$-$\omega$ model gives a good estimate of the jet's width while the two RNG formulations overestimate it. The corresponding profiles predicted by the $k$-$\varepsilon$-wf and $k$-$\varepsilon$-enh formulations (not shown here for lack of space) are essentially identical. In these two cases the underprediction of the peak jet velocity and overestimation of its width is more important than in Figure 7(c). The negative velocities in the lower third of the cavity predicted by these two standard $k$-$\varepsilon$ formulations are however in closer agreement with the measured values than the results in Figure 7(c). The corresponding LES predictions by Davidson and Nielsen (1996) give a good estimate of the maximum jet velocity but overestimate the extent of the region with positive velocities. They also overestimate the magnitude of the negative velocities for $y/H < 0.2$.

In view of these comparisons between experimental values, the present numerical results and those by Davidson and Nielsen (1996) we conclude that there is no advantage in using LES with a much denser grid for the flow under consideration. For engineering problems, such as HVAC applications, any of the two equations models investigated in this paper provide acceptable results.

Figure 8 shows the profiles of the horizontal velocity component at $z/W = -0.4$ and $x/H = 2$. It should be noted that the measured values are very different from those in the symmetry plane (Figure 7(c)). Therefore, the flow field is not 2D as assumed in some previous studies. The $k$-$\varepsilon$-enh formulation underestimates considerably the maximum positive velocity near the top wall while the $k$-$\varepsilon$-RNG-enh gives the best estimate of this quantity. However, all three formulations overestimate the distance of this maximum value from the top wall. The position of zero velocity slightly below the midheight of the cavity is best predicted by the $k$-$\varepsilon$-enh formulation. On the other hand, in the lowest fifth of the cavity where the most important negative velocities have been measured, the best results are obtained by the SST-$k$-$\omega$ formulation.

It is quite evident that in the case of this isothermal flow the two models using the enhanced wall treatment do not predict identical results, as was the case for the natural convection flow analysed in Section 4.1. This indicates that the level of turbulent intensity is in the present case considerable. Therefore, the one equation model of Wolfstein (1969) is not applied far from the wall as was the case for the natural convection flow.

*4.2.2 Turbulence quantities*. There are no experimental data for turbulent quantities in the study by Nielsen *et al.* (1978). We therefore simply present in Figure 9 the kinetic energy contours at the meridian plane ($z/W = 0$) for three formulations: $k$-$\varepsilon$-enh,

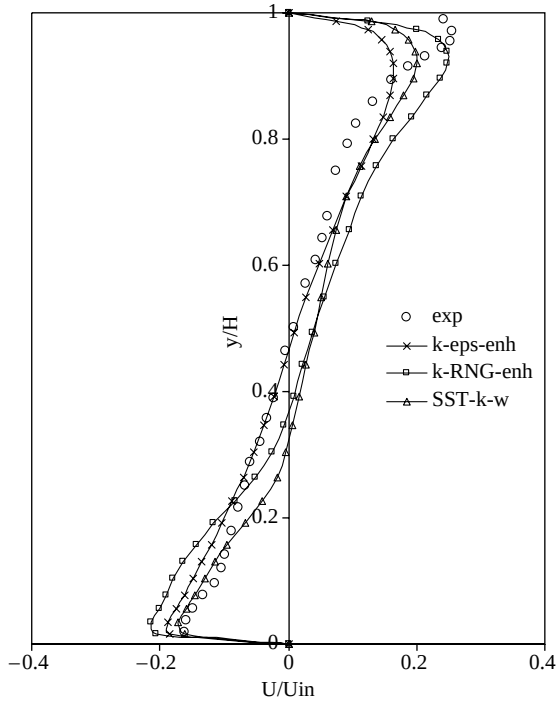


**Figure 8.**
Horizontal velocity profiles at $z/W = -0.4$ and $x/H = 2$ (isothermal flow)

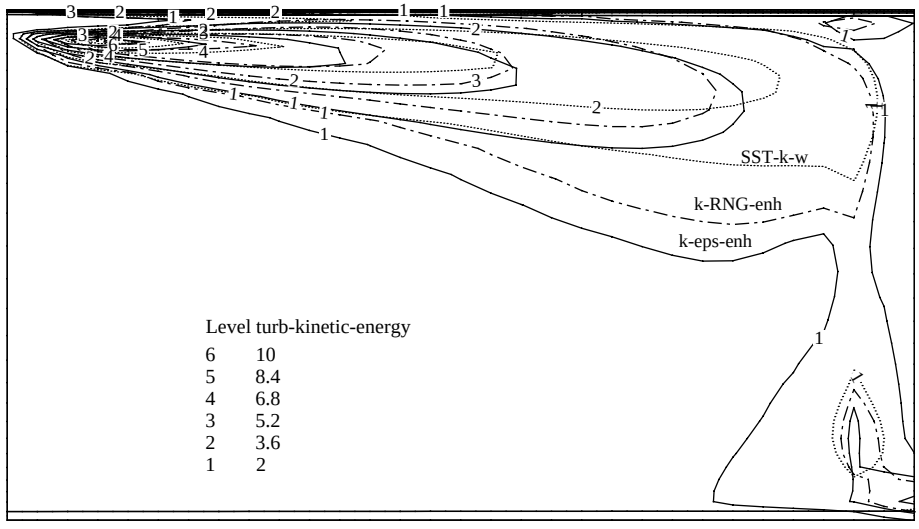


**Figure 9.**
Iso-$k$ contours at $z/W = 0$ (isothermal flow)

$k$-$\varepsilon$-RNG-enh and SST-$k$-$\omega$. Qualitatively the models predict the same behaviour. The turbulent kinetic energy is maximum near the air inlet (top left region of the cavity) where the velocity gradient is highest (Figure 7(a) and (b)) and decreases as the flow approaches the wall at $x/H = 1$. Nevertheless, two zones of fairly important turbulent kinetic energy are present near the top and bottom of this wall. The former is associated with the anti-clockwise vortex predicted by all five formulations in the upper right corner of the cavity. The latter is attributed to the high-velocity gradients present in the lower right corner resulting from the combined effects of the flow acceleration near the outlet and the backwards flow (Figure 7(c)). On the other hand, the quantitative agreement of these predictions is poor. The $k$-$\varepsilon$-enh formulation predicts the largest turbulent kinetic field followed by the $k$-$\varepsilon$-RNG-enh and SST-$k$-$\omega$. The important differences between the predicted positions of the iso-$k$ contours clearly indicate that it is difficult to reproduce details of the turbulent quantities with two equation turbulence models. This limitation has been noted in several previous studies (Peng and Davidson, 2000; Joubert *et al.*, 2005) and illustrates the need of higher order models for the prediction of turbulent quantities.

## 5. Conclusion

Turbulent natural convection in an air filled 2D cavity and isothermal turbulent forced flow in a ventilated cavity were analysed numerically with three different two-equation models.

The natural convection case was modelled taking into account heat conduction in the horizontal walls which has an important effect on the air temperature near these walls. The grid independence tests based on the turbulent kinetic energy profiles, rather than the less sensitive mean quantities, showed that a $30 \times 30$ grid provides a good compromise between accuracy and computer memory. The best predictions of the mean air temperature distribution were obtained with the two $k$-$\varepsilon$ models associated with standard wall functions. On the other hand, the best results for the mean velocity profile were obtained with the SST-$k$-$\omega$ model followed by the two $k$-$\varepsilon$ models associated with the enhanced wall treatment. The best predictions of the mean temperature profile at $x/H = 0.5$ were obtained with the $k$-$\varepsilon$-wf and SST-$k$-$\omega$ models. The performance of all these two-equation models with regard to the prediction of turbulence quantities is rather poor even though they are in good agreement with previous LES results. In conclusion we believe that the near-wall treatments used in the present study need further improvement. This is particularly true for the wall functions approach.

It was noted that comparisons of measured and calculated quantities at mid-height of the natural convection cavity are not sufficient to establish the validity of models and fully describe all the phenomena present in the cavity. The effect of flow along the horizontal walls and the four corners of the cavity are not captured with equal sensitivity by the different models which tend to underestimate the air temperature in the lower half of the cavity and overestimate it in the upper half.

In the case of the isothermal forced flow the enhanced wall treatment was more successful in describing near-wall effects. In the core region of the flow the $k$-$\varepsilon$-RNG model with enhanced wall treatment produced satisfactory results. The predictions of the SST-$k$-$\omega$ model were generally in good agreement with experimental data while the $k$-$\varepsilon$ model overestimated the thickness of the jet.

If the two types of flow are considered the performance of the models under evaluation is more or less equivalent. The prediction of mean velocities and temperatures is always satisfactory for engineering applications such as HVAC calculations. On the other hand, the prediction of turbulent quantities is less precise. The near wall formulations which perform better for one type of flow are less successful for the other type.

## References

Ampofo, F. and Karayiannis, T.G. (2003), "Experimental benchmark data for turbulent natural convection in an air filled square cavity", *Int. J. of Heat and Mass Transfer*, Vol. 46 No. 19, pp. 3551-72.

Aounallah, M., Belkadi, M., Adjlout, L. and Imine, O. (2005), "Computation of turbulent buoyant flows in enclosures with low-Reynolds-number $k$-$\omega$ models", *Heat and Technology*, Vol. 23 No. 2, pp. 123-9.

Bellache, O., Ouzzane, M. and Galanis, N. (2005), "Coupled conduction, convection, radiation heat transfer with simultaneous mass transfer in ice rinks", *Numerical Heat Transfer: Part A – Applications*, Vol. 48 No. 3, pp. 219-38.

Chen, Q. (1995), "Comparison of different $k$-ε models for indoor airflow computations", *Numerical Heat Transfer, Part B: Fundamentals.*, Vol. 28, pp. 353-69.

Chen, Q. (1996), "Prediction of room air motion by Reynolds-stress models", *Building and Environment*, Vol. 31 No. 3, pp. 233-44.

Chen, Q. and Xu, W. (1998), "Zero-equation turbulence model for indoor airflow simulation", *Energy and Buildings*, Vol. 28 No. 2, pp. 137-44.

Davidson, L. and Nielsen, P.V. (1996), "Large Eddy simulations of the flow in a three-dimensional ventilated room", *5th Int. Conf. on Air Distribution in Rooms, Roomvent, Yokohama*, Vol. 2, pp. 161-8.

Dechang, W., Guangsheng, D. and Jingyi, W. (2005), "Numerical experimental study on the 3-D flow field around a van with a dome for energy saving", *Energy Conversion and Management*, Vol. 46 No. 6, pp. 833-46.

Dol, H.S. and Hanjalic, K. (2001), "Computational study of turbulent natural convection in a side-heated near-cubic enclosure at a high Rayleigh number", *Int. J. of Heat and Mass Transfer*, Vol. 44 No. 12, pp. 2323-44.

Fluent (2005), *Fluent 6 User's Guide*, Fluent Inc., Lebanon, NH.

Holling, M. and Herwig, H. (2005), "Asymptotic analysis of the near-wall region of turbulent natural convection flows", *Journal of Fluid Mechanics*, Vol. 541, pp. 383-97.

Joubert, P., LeQuere, P., Beghein, C., Collignan, B., Couturier, S., Glockner, S., Groleau, D., Lubin, P., Musy, M., Sergent, A. and Vincent, S. (2005), "A numerical exercise for turbulent natural convection and pollutant diffusion in a two-dimensional partially partitioned cavity", *Int. J. of Thermal Sciences*, Vol. 44 No. 4, pp. 311-22.

Kader, B. (1981), "Temperature and concentration profiles in fully turbulent boundary layers", *Int. J. of Heat and Mass Transfer*, Vol. 24 No. 9, pp. 1541-4.

Launder, B.E. and Spalding, D.B. (1974), "The numerical computation of turbulent flows", *Computer Methods in Applied Mechanics and Engineering*, Vol. 3, pp. 269-89.

Liu, F. and Wen, J.X. (1999), "Development and validation of an advanced turbulence model for buoyancy driven flows in enclosures", *Int. J. of Heat and Mass Transfer*, Vol. 42 No. 21, pp. 3967-81.

Menter, F.R. (1993), "Zonal two equation $k$-$\omega$ turbulence models for aerodynamic flows", AIAA Paper 93-2906.

Menter, F.R., Kuntz, M. and Langtry, R. (2003), "Ten years of experience with the SST turbulence model", in Hanjalic, K., Nagano, Y. and Tummers, M. (Eds), *Turbulence, Heat and Mass Transfer*, Vol. 4, Begell House Inc., Redding, CT, pp. 625-32.

Mora, L., Gadgil, A.J. and Wurtz, E. (2003), "Comparing Zonal and CFD model predictions of isothermal indoor airflows to experimental data", *Indoor Air*, Vol. 13, pp. 77-85.

Nielsen, P.V., Restivo, A. and Whitelaw, J.H. (1978), "Velocity characteristics of ventilated rooms", *ASME J. of Fluids Eng.*, Vol. 100 No. 3, pp. 291-8.

Omri, M. and Galanis, N. (2006a), "Numerical analysis of turbulent natural convection in a cavity", *Proceedings (CD) 13th Int. Heat Transfer Conf., Sydney, Australia*.

Omri, M. and Galanis, N. (2006b), "Numerical analysis of turbulent forced convection in a cavity", *Proceedings (CD) CSME Forum, University of Calgary, Calgary, Canada*.

Peng, S-H. and Davidson, L. (1988), "Computation of turbulent buoyant flows in enclosures with low-Reynolds-number $k$-$\omega$ models", *Doktorsavhandlingar vid Chalmers Tekniska Hogskola*, Vol. 1391, pp. 1-23.

Peng, S-H. and Davidson, L. (2000), "Numerical investigation of turbulent buoyant flow in a cavity using large eddy simulation", in Nagano, Y., Hanjalic, K. and Tsuji, T. (Eds), *Turbulence Heat and Mass Transfer*, Vol. 3, pp. 737-44.

Peng, S-H. and Davidson, L. (2001), "Large eddy simulation for turbulent buoyant flow in a confined cavity", *Int. J. of Heat and Fluid Flow*, Vol. 22 No. 3, pp. 323-31.

Posner, J.D., Buchanan, C.R. and Dunn-Rankin, D. (2003), "Measurement and prediction of indoor air flow in a model room", *Energy and Building*, Vol. 35, pp. 515-26.

Quéré, S., Galli, A., Benay, R. and Bur, R. (2003), "Validation d'un modèle $k$-faiblement non-linéaire", paper presented at 16e Congrès Français de Mécanique, Nice.

Shpak, S.I. (1994), "Model of turbulent viscosity for computation of three-dimensional turbulent boundary layers", *Journal of Applied Mechanics and Technical Physics*, Vol. 35 No. 6, pp. 898-905.

Speziale, C.G., Abid, R. and Anderson, E.C. (1992), "Critical evaluation of two-equation models for near-wall turbulence", *AIAA Journal*, Vol. 30 No. 2, pp. 324-31.

van Leer, B. (1979), "Toward the ultimate conservative difference scheme. IV. A second order Sequel to Godunov's method", *Journal of Computational Physics*, Vol. 32, pp. 101-36.

Wilcox, D.C. and Traci, R.M. (1976), "A complete model of turbulence", AIAA Paper 76-351.

Wolfstein, M. (1969), "The velocity and temperature distribution of one-dimensional flow with turbulence augmentation and pressure gradient", *Int. J. of Heat and Mass Transfer*, Vol. 12, pp. 301-18.

Yakhot, V. and Orszag, S.A. (1986), "Renormalization group analysis of turbulence: I. basic theory", *Journal of Scientific Computing*, Vol. 1 No. 1, pp. 1-51.

Yakhot, V., Orszag, S.A., Thangam, S., Gatshi, T.B. and Speziale, C.G. (1992), "Development of a turbulence model for shear flow by a double expansion technique", *Physics of Fluids. A, Fluid Dynamics*, Vol. 4, pp. 1510-20.

## Further reading

Peng, S-H. and Davidson, L. (2002), "On a subgrid-scale heat flux model for large eddy simulation of turbulent thermal flow", *Int. J. of Heat and Mass Transfer*, Vol. 45 No. 7, pp. 1393-405.

Sun, Y., Tan, Z., Zhang, Y. and Zhao, L. (2004), "Comparison of Six CFD models for room airflow study with PIV measurement data", Paper number 044097, ASAE Annual Meeting, American Society of Agricultural and Biological Engineers, St. Joseph, MI.

## Corresponding author

Nicolas Galanis can be contacted at: nicolas.galanis@usherbrooke.ca